Anomalous interaction of strong laser radiation with dense plasma

N. G. Basov, O. N. Krokhin, V. V. Pustovalov, A. A. Rupasov, V. P. Silin, G. V. Sklizkov, V. T. Tikhonchuk, and A. S. Shikanov

P. N. Lebedev Physics Institute, USSR Academy of Sciences
(Submitted February 13, 1974)
Zh. Eksp. Teor. Fiz. **67**, 118-133 (July 1974)

Results are reported of an experimental and theoretical study of the interaction of light fluxes of 2×10^{12}–2×10^{13} W/cm^2 from a neodymium laser with aluminum and polyethylene targets. Three effects are considered: almost total absorption of the laser radiation by the plasma, oscillations in the intensity of the weak reflected signal as a function of time, and generation of laser-radiation harmonics by the plasma. It is shown that the light fluxes used in this work are in excess of the threshold values which, according to the theory of parametric resonance, are necessary for the development of parametric instability in laser plasma. The observed phenomena are interpreted in terms of the theory of parametric resonance in plasma and the theory of parametric turbulence. It is noted that measurements of the period and modulation depth of the oscillating light intensity reflected by the plasma are important for laser plasma diagnostics.

INTRODUCTION

The idea of producing controlled thermonuclear reactions with positive energy yield in dense plasmas exposed to strong laser radiation[1,2] is currently being developed in a number of different ways. The complexity of the problem is such that it can be approached in its entirety only by numerical simulation on modern computers.[3-5] On the other hand, individual aspects of this problem are fully accessible to both experimental and theoretical (analytic) investigation. One such important aspect of the problem of laser-driven controlled thermonuclear reaction, namely, the absorption and reflection of strong radiation by laser plasma, is considered in the present paper.

Simple estimates of the energy yield of a thermonuclear reaction, which it is believed should develop in laser plasma heated by light,[1-5] indicate that the efficiency of absorption of laser radiation is important in this process. In this sense, the attainment of optimum energy transfer between strong beams of radiation and laser plasma, i.e., the production of plasma with the necessary parameters at minimum laser energy, is at present the immediate problem. The first step in solving it is to investigate the physics of absorption of the kind of light fluxes which can be produced at the present time.[6-8]

This paper is a continuation of previously published experimental studies of the reflection coefficient for nanosecond pulses produced by a neodymium laser[9,10] in the flux range 2×10^{12} – 2×10^{13} W/cm^2.

1. APPARATUS

The experiment is illustrated schematically in Fig. 1. We use a neodymium glass laser consisting of a master generator 1, pulse shaper 2, 3, and three amplifying stages 4, 5. The generator was Q-switched. To improve contrast (ratio of pulse to background energy) the radiation flux from the generator was twice passed through a Kerr cell 3 controlled by a laser-triggered discharge gap 2. To reduce the target-laser coupling, i.e., to eliminate the free-generation background preceding the

main light pulse, the vacuum chamber 8 containing the target was placed at a distance of about 8 m from the end of the last amplifier. Moreover, transmission filters acting as efficient decouplers were placed before the second and third amplifiers. As a result, the laser produced pulses with $\tau \approx 3$—4 nsec (at half height), energy of up to 10 J, contrast not worse than 10^{-5}, and beam divergence $\sim 10^{-3}$ rad. The light-beam diameter on the lens with focal length 5.5 cm was 2.5 cm. The radiation flux incident on the target was varied by introducing calibrated neutral light filters into the beam.

The energy and shape of the incident and reflected pulses was recorded by calorimeters 9 and coaxial photocells 7 (type FÉK-09). Signals from these photocells were fed into a six-beam oscillograph 6LOR-02-1 which can simultaneously record a number of fast processes. The high time resolution used to investigate the incident and reflected pulses was achieved by the utilization of the photoelectric recorder 11 (type FER-2) The image on the screen of this recorder was photographed by the camera 12. The time resolution of the
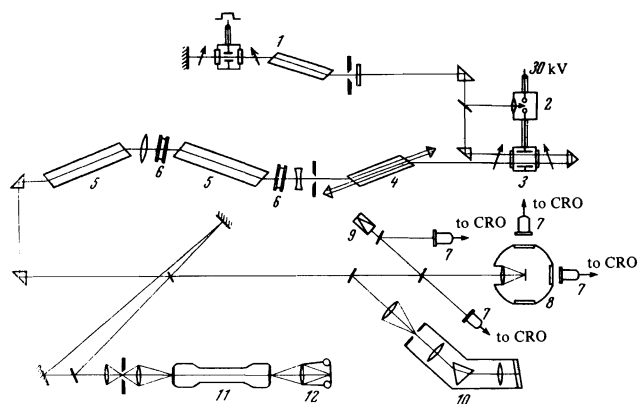

FIG. 1. Schematic arrangement of the apparatus: 1—Q-switched neodymium laser incorporating a Kerr cell, 2—laser controlled discharge gap, 3—pulse-shaping Kerr cell, 4—three-transit amplifier, 5—second and third amplifiers, 6—transmission filter, 7—coaxial photocells, 8—working chamber, 9—calorimeter, 10—prism spectrograph, 11—photoelectric recorder (FER-2), 12—photographic camera.

system was better than 10^{-10} sec. The spectral composition of the reflected radiation was investigated with the aid of the prism spectrograph 10. The dispersion in the region of the second harmonic of the neodymium radiation (5300 Å) was 20 Å/mm.

2. REFLECTION COEFFICIENT OF DENSE LASER PLASMA

The reflection coefficient R was measured as a function of the incident flux density for solid aluminum and polyethylene $[(CH_2)_n]$ targets. The reflection coefficient is defined as the ratio $R = \epsilon_{ref}/\epsilon_{inc}$ where ϵ_{ref} is the energy reflected from the plasma into the aperture of the focusing lens and ϵ_{inc} is the laser radiation energy incident on the plasma.

Figure 2 illustrates the measured reflection coefficient R integrated over the pulse as a function of the flux density q incident on the aluminum target. The radiation flux density q is defined, as usual, as the ratio of the energy ϵ_{inc} in the light beam incident on the plasma to its pulse length τ and area S of the focal spot, i.e., $q = \epsilon_{inc}/\tau S$. As can be seen from the figure, the reflection coefficient R decreases monotonically from $R \approx 1\%$ at flux densities of the order of 2×10^{12} W/cm^2 down to about 0.3% for the flux density of 2×10^{13} W/cm^2.

Figure 3 shows the reflection coefficient as a function of the flux density for the polyethylene target in the same range of values of q. As can be seen, the reflection coefficient remains practically constant and amounts to about 1%.

The small absolute value of the measured reflection coefficient of plasma for strong laser radiation and, in particular, the reduction in the reflection coefficient with increasing flux density, does not fit into the framework of the usual theories of absorption and reflection of beams of light, based on Coulomb collisions between plasma electrons and ions (collisional absorption) and the skin effect for electromagnetic waves with frequency less than the plasma frequency. In point of fact, when the plasma electron temperature is $T_e \approx 1$ keV, which was probably realized in our experiments, the optical thickness of the plasma for collisional absorption is small in comparison with unity (the plasma is transparent) and amounts to 0.3—0.03 for a characteristic size of plasma density inhomogeneities a = 0.01—0.001 cm. We shall therefore report data on parametric effects produced in plasma by strong radiation and

capable of explaining the nonclassical (i.e., anomalous) interaction of radiation with plasma.

To justify the application of the idea of parametric resonance to the interpretation of laser experiments in general and those described here in particular, we must first compare the characteristic times and fluxes in the experiment, on the one hand, and those necessary for the development of parametric instability and turbulence, on the other. With this aim in view, we summarize below the formulas for threshold fluxes q_{th} (in W/cm^2) and maximum growth rates γ_{max} (in nsec^{-1}) for the five most characteristic parametric instabilities in isotropic homogeneous plasma exposed to strong radiation (see, for example,[11-17]):

1) aperiodic instability $(t \rightarrow l + a)$:

$$q_{th} = 6.7 \cdot 10^{12} (z + T_i/T_e) T_e^{-1/2} \Lambda_1, \quad \gamma_{max} = 2.4 \cdot 10^{-7} (z + T_i/T_e)^{-1/2} z (AT_e)^{-1/2} q^{1/2}.$$

2) decay into ion-acoustic and plasma waves $(t \rightarrow l + s)$:

$$q_{th} = 1.9 \cdot 10^{11} z^{1/2} (AT_e)^{-1/2} \Lambda_1, \quad \gamma_{max} = 10^{-6} (z/A)^{1/2} T_e^{-1/2} q^{1/2};$$

3) decay into two plasmons $(t \rightarrow l + l)$:

$$q_{th} = 1.2 \cdot 10^{11} z^2 T_e^{-3} \Lambda_1^2, \quad \gamma_{max} = 2.4 \cdot 10^{-7} q^{1/2};$$

4) SMBS $(t \rightarrow t + s)$:

$$q_{th} = 2.3 \cdot 10^{-10} n_e z^{1/2} (AT_e)^{-1/2} \Lambda_2, \quad \gamma_{max} = 2.6 \cdot 10^{-8} (z/A)^{1/2} T_e^{1/2} q^{1/2} (1 - 10^{-21} n_e)^{1/2};$$

5) SRS $(t \rightarrow t + l)$:

$$q_{th} = 1.6 \cdot 10^{-9} z^2 n_e T_e^{-3} F(x) \Lambda_2^2, \quad \gamma_{max} = 0.9 \cdot 10^{-17} n_e^{1/2} q^{1/2} (x - 1)^{-1} F^{-1/2}(x).$$

In these expressions

$$F = (x-1)^{-1} [(x^2-1)^{1/2} + [x(x-2)]^{1/2}]^{-2},$$

$$x = 3.16 \cdot 10^{10} n_e^{-1/2}, \quad \Lambda_1 = 1 + 0.3 \lg T_e, \quad \Lambda_2 = 1 + 0.3 \lg (10^{10} n_e^{-1/2} T_e),$$

where T_e is in keV and n_e in cm^{-3}.

The first three decays correspond to parametric generation of longitudinal (potential) plasma oscillations by the light wave, which are absorbed by particles (electrons and ions) not only as a result of Coulomb collisions, but also through the inverse Cerenkov effect, and cannot directly leave the plasma. It is precisely this instability which ensures absorption of light in addition to collisional absorption. On the other hand, the last two instabilities (SMBS and SRS) are of completely different origin and have a scattering character. The basic physics of the situation in this case is that the strong light wave incident on the plasma generates not only the potential oscillations (sound and plasmon, respectively), but also a light wave which freely leaves the plasma which is transparent for Coulomb collisions. The appearance of any of the five parametric instabilities results in an anomalous interaction between radiation and laser plasma. There is, however, one important difference between them: the first three determine the anomalous absorption of light by the plasma, and the last two determine the anomalous scattering ("reflection").

It is clear from the above formulas that for plasma densities $n_e \lesssim 10^{21}$ cm^{-3}, electron temperatures $T_e \approx 0.1-1$ keV, and pulse lengths $\tau \gtrsim 1$ nsec, at least one of the above five parametric instabilities will appear and will fully succeed in developing if the light flux q is not less than $2 \times 10^{12} - 2 \times 10^{13}$ W/cm^2, as was indeed the case in our experiments. This situation is characteristic, however, only for homogeneous unbounded plasma when any of the waves generated parametrically
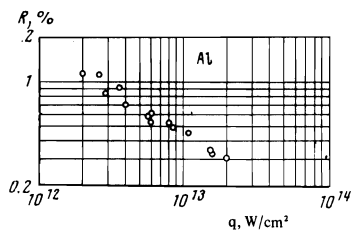
FIG. 2. Experimental reflection coefficient R integrated over the pulse of neodymium-laser radiation reflected into the solid angle of the focusing lens as a function of the incident flux density q on the aluminum target.
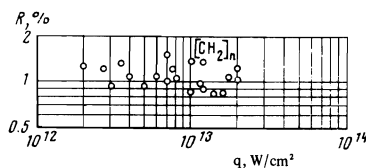
FIG. 3. Same as Fig. 2 for the polyethylene target.

N. G. Basov et al.

Conditions under which the effect of plasma inhomogeneity on the thresholds for parametric instabilities in plasma heated by neodymium laser radiation can be neglected

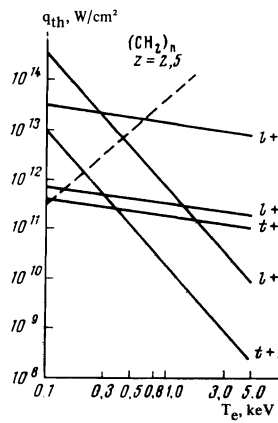| Instability	a, cm		
	Arbitrary target	$(CH_2)_n$ target	Al target
$t \to l + a$	$\gtrsim 6 \cdot 10^{-3} T_e^2 z^{-1}$	$\gtrsim 2 \cdot 10^{-3} T_e^2$	$\gtrsim 6 \cdot 10^{-1} T_e^2$
$t \to l + s$	$\gtrsim 0.7 \, T_e^3 T_i^{-1} z^{-2} A^{-1/4}$	$\gtrsim 4 \cdot 10^{-2} \, T_e^{7/4}$	$\gtrsim 10^{-3} T_e^{7/4}$
$t \to l + l$	$\gtrsim 2.5 \cdot 10^{-2} \, T_e^2 z^{-1}$	$\gtrsim 8.5 \cdot 10^{-3} \, T_e^2$	$\gtrsim 2.5 \cdot 10^{-3} T_e^2$

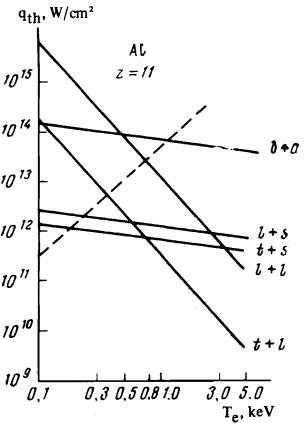FIG. 4   FIG. 5

FIG. 4. Theoretical light flux necessary for the excitation of the five parametric instabilities as a function of the electron temperature in the polyethylene laser plasma (solid curves). Broken line shows $T_e \sim q^{4/9}$.

FIG. 5. Same as in Fig. 4 for the aluminum laser plasma ($z = 11$, $A = 27$).
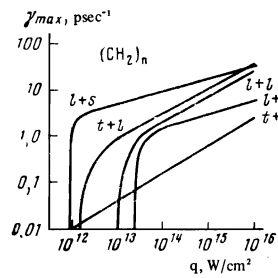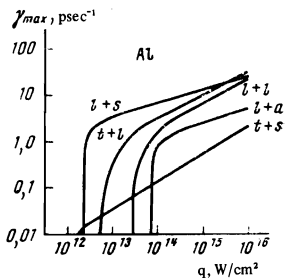

FIG. 6   FIG. 7

FIG. 6. Theoretical maximum growth rate γ_{max} for the parametric excitation of instabilities in polyethylene laser plasma as a function of the incident flux density q. The sharp fall in the growth rates and their subsequent fall to zero at the threshold flux was calculated from the formulas characterizing the near-threshold region of parametric excitation.

FIG. 7. Same as in Fig. 6 for aluminum laser plasma.

in the plasma (sound, plasmon, or light) remain in the plasma.

It is important to emphasize in this connection that when the finite size of the real laser plasma and its inhomogeneity are taken into account, this does not affect the above description of the anomalous interaction of light with plasma as applied to the first three parametric instabilities governing the anomalous absorption for the light fluxes employed in our experiments. In point of fact (see, for example, page 179 in[12]), plasma inhomogeneity with characteristic linear size a increases the threshold for such parametric instabilities if a is much less than the electron mean free path for Coulomb collisions with ions, multiplied by the logarithm of ratio of the light and collision frequencies. In our experiments, such a stringent inequality cannot be satisfied because when $T_e \approx 1$ keV and $n_e \approx 10^{21}$ cm^{-3} the thermal velocity is $v_{Te} \approx 10^3$ cm/sec, $\nu_{ei} \approx 10^{12}$ sec^{-1}, and the mean free path is about 10^{-3} cm, i.e., for $a \approx 10^{-2}$ cm the effect of inhomogeneity on the threshold is unimportant. This estimate is improved in the Table which gives more detailed conditions that must be satisfied if the influence of inhomogeneity is to be negligible[12,17] (z is the ion charge, A is the atomic number of the target, and T_e and T_i are the electron and ion temperatures in keV). Because of the unimpeded escape from the inhomogeneous laser plasma of the unstable (scattered) light wave, the SMBS and SRS instabilities are much more influenced by density inhomogeneities which increase their threshold to values exceeding those employed in our experiments.

The threshold fluxes and maximum growth rates for the aperiodic parametric instability ($t \to l + a$) and the decay of the light wave into electron Langmuir and ion-acoustic oscillations ($t \to l + s$) are given above for densities n_e approaching the critical value $n_{crit} \approx 10^{21}$ cm^{-3} for the neodymium laser. The ($t \to l + l$) instability involving the decay of the light wave into two electron Langmuir oscillations develops at densities $n_e \approx 7.5 \times 10^{20}$ cm^{-3} equal to $0.25 \, n_{crit}$. The two other instabilities, namely, SMBS for neodymium radiation on ion-acoustic oscillations ($t \to t + s$) and SRS on electron Langmuir oscillations ($t \to t + l$) are excited in a broad range of plasma densities.

The above formulas for q_{th} determine the dependence of the threshold light fluxes on the electron and ion temperatures T_e and T_i of the laser plasma, the ion charge z, and the atomic number A of the target. The electron temperature dependence of the threshold fluxes for the parametric excitation of waves in dense laser plasmas is illustrated graphically in Fig. 4 (polyethylene target) and Fig. 5 (aluminum target). The broken straight line represents the temperature of the laser plasma ($T_e \sim q^{4/9}$) as a function of the flux of neodymium radiation on the target. It is clear that the range of homogeneous laser-plasma parameters for

which parametric excitation of the first two instabilities is possible lies on the broken straight lines in Figs. 4 and 5 to the right of the intersection of this line with the line showing the instability threshold as a function of temperature.

Curves corresponding to SMBS and SRS are useful only for uniform unbounded plasma. The graphs showing the threshold fluxes as functions of temperature for the $t \to t + s$ and $t \to t + l$ instabilities are shown in Figs. 4 and 5 for electron densities in homogeneous plasma $n_e \approx 5 \times 10^{20}$ cm^{-3} and $n_e \approx 10^{20}$ cm^{-3}. We note also that the threshold fluxes for the parametric excitation of instability increase with increasing ion charge in the plasma.

Figures 6 and 7 show the maximum growth rates of parametric excitation as functions of the light fluxes incident on the polyethylene and aluminum laser plasmas in a broad range between $q = q_{th}$ and $q \gg q_{th}$. We emphasize that the $\gamma_{max}(q)$ curves in Figs. 6 and 7 take into account the fact that the electron temperature is $T_e \sim q^{4/9}$ which is specific for laser plasma. The growth rates for the $t \to t + s$ and $t \to t + l$ instabilities are calculated for the same densities of homogeneous plasma as the threshold fluxes in Figs. 4 and 5.

The effectiveness of any particular mechanism of absorption of light by laser plasma is characterized by its contribution to the optical depth of the plasma. In the case of collisional absorption (with Coulomb collision frequency ν_i at the critical point) the optical depth of the laser plasma with characteristic inhomogeneity size a is determined by a quantity close to $a\nu_{ei}/c$, where c is the velocity of light in vacuum. The anomalous absorption, which is due to the development of parametric turbulence in the laser plasma, is characterized by the effective frequency ν_T of light absorption, which may substantially exceed the Coulomb frequency, i.e., $\nu_T \gg \nu_{ei}$ (see[18]). Moreover, it is important to remember that in the near-threshold range of flux densities, and despite the high effective frequency $\nu_T \gg \nu_{ei}$, the contribution of anomalous absorption to the optical depth may turn out to be comparable with, or even less than, the collisional contribution because of the narrow range of values of the difference between the laser frequency and the electron Langmuir frequency. In fact, in contrast to collisional absorption, anomalous absorption with frequency ν_T occurs in the small region $\beta a < x < 0$ of the density profile $n_e = n_{crit}(1 + x/a)$ in the plasma, which corresponds to the detuning $\omega_0 - \omega_{Le} = \omega_0[1 - (1 - \beta)^{1/2}] \ll \omega_0$ for $\beta \ll 1$, so that the contribution $2\beta^{1/2}a\nu_T/c$ of the parametric turbulence to the optical thickness is not small in comparison with the collisional contribution $a\nu_{ei}/c$ only if $\nu_T \gtrsim \nu_{ei}/2\beta^{1/2} \gg \nu_{ei}$.

In the near-threshold region of parametric excitation $q \gtrsim q_{th}$ the effective frequency $\nu_T \approx 2\bar{\gamma}(q/q_{th} - 1)$ is large in comparison with the Coulomb frequency ν_{ei} if the Landau damping γ of plasma waves is not small, i.e., $\bar{\gamma} \gg \nu_{ei}$ (see[18]). Under these conditions, anomalous absorption occurs in two simultaneous stages, namely, the parametric resonance consists of the nonlinear transformation of light into a plasma wave which is absorbed by electrons with frequency $\bar{\gamma}$ through the Cerenkov effect. When $q \gg q_{th}$ (q of the order of 10^{14} W/cm^2 or more), the conditions for the dominance of turbulent parametric absorption over collisional absorption are improved, since there is then an increase in the effective frequency $\nu_T \approx 2\bar{\gamma}(q/q_{th})^{1/2}$ and an expansion of the detuning interval within which parametric resonance can occur.

In the case of nonlinear absorption, $\nu_T \approx \nu_{ei}(q/q_{th})^{1/2}$, we must remember that the reduction in the flux as a function of the optical depth takes the power-law form

$$q = q_0[1 + (a\nu_{ei}/2c)(q_0/q_{th})^{1/2}]^{-2},$$

rather than an exponential form (q_0 is the light flux incident on the plasma).

In our experiments, i.e., for relatively low flux densities $q \approx 2 \times 10^{12} - 2 \times 10^{13}$ W/cm^2, when $q/q_{th} - 1 \sim 1$, the optical thickness due to the anomalous absorption for $\omega_0 - \omega_{Le} \approx 0.1\,\omega_0$ is not less than the contribution due to the collisional process in the plasma with temperature of the order of 0.5—0.8 keV. The heating of the target to a temperature of the order of a few hundred electron volts occurs as a result of the collisional absorption of the light flux, i.e., due to Coulomb collisions between electrons and ions with frequency ν_{ei}. Next, as the temperature T_e increases, the plasma should become transparent ($\nu_{ei} \sim T_e^{-3/2}$) and the reflection coefficient should increase with increasing flux q in the absence of anomalous absorption. Experiment shows, however, (see Figs. 2 and 3) that in

practice the reflection coefficient R does not increase with increasing flux (and for the aluminum target it even decreases). It is this fact that enables us to conclude that, in hot laser plasma ($T_e > 0.5$ keV), collisional absorption is to a large extent replaced by an anomalous absorption which is more effective under these conditions and is due to parametric turbulence which develops for light fluxes of the order of those used in these experiments.

In addition to the weak and flux-dependent reflection, another manifestation of anomalous interaction between strong laser radiation and dense plasma is the time modulation of the reflected light intensity, which is described in the next section and is interpreted in terms of the theory of parametric turbulence.

3. MODULATION OF REFLECTED INTENSITY AS A FUNCTION OF TIME

For incident light-flux densities $q > 10^{12}$ W/cm^2, the signal reflected by the plasma was found to be amplitude-modulated on some oscillograms with a period of about 0.5 nsec. This undoubtedly confirms that the reflected intensity is modulated because when a coaxial photocell receives a light pulse with leading edge shorter than the time resolution of the system, the result is a "ring" in the recording system, which modulates the electrical signal (it was noted in[9] that the leading edge of the reflected light signal is in fact shortened). The question as to whether the measured modulation of the electrical signal is an instrumental or a true physical effect characterizing the anomalous interaction between light and laser plasma can only be answered by using a recording system with a time resolution much shorter than the length of the leading edge of the pulse. We have therefore employed an electrooptical converter to record the reflected signal.

To ensure high time resolution, we used a photoelectric recorder (type FER-2) with electrooptical converter UMI-92, which ensured a resolution of better than 10^{-10} sec for a 32 nsec scan and slit width of 100 μm. This is higher by an order of magnitude than the time resolution in the case of oscillographic recording.

Both the reflected and the incident radiation was focused by a cylindrical lens on the entrance slit of a photochronograph equipped with a nine-step attenuator. The incident signal was optically delayed by about 10 nsec relative to the reflected signal. In this way, both the incident and the recorded signals were recorded on the same time scan. The presence of the nine-step attenuator enabled us to use normal blackening on the photographic film for at least two of the attenuated steps for each scan.

The measurements were performed for $q \approx 7 \times 10^{12}$ W/cm^2 on the aluminum target. Figure 8 shows a characteristic time scan. Figure 9 gives the incident and reflected intensities as functions of time for the scan shown in Fig. 8.

Analysis of a large number of such records gave the following results. The width of the leading front of the reflected signal is reduced in all cases by a factor of roughly 2—3 as compared with the incident pulse (length ~1.5 nsec). For all pulses, the reflected signal shows intensity beats with modulation depth up to 30—50% of the maximum. The period of these beats is on the aver-
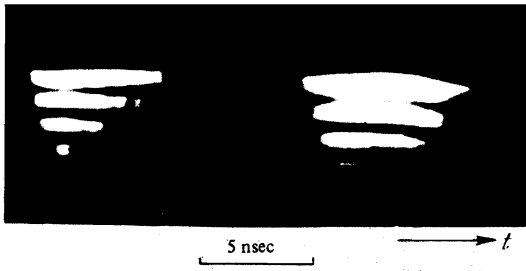
FIG. 8. Characteristic scan of the incident (right) and reflected (left) laser radiation obtained with the nine step attenuator.
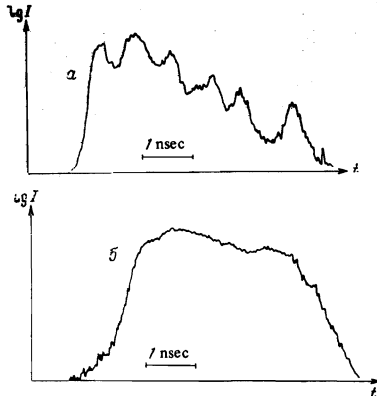

FIG. 9. Reflected (a) and incident (b) signals as functions of time for the scan shown in Fig. 8.

age 0.6 ± 0.1 nsec. In 40% of all cases, the incident signal also shows individual but much weaker flux bursts which either coincide with the beats on the reflected signal (10% of all cases) or do not coincide with any of the beats (30% of all cases).

The experimental results thus enable us to suggest that the deep modulation of the reflected light pulse is a physical effect due to the nonlinear interaction between the strong light flux and the laser plasma. The non-linearity of the effect is clearly seen, above all, in its threshold properties: the oscillations on the reflected flux are observed only for incident fluxes $q \gtrsim 10^{12}$ W/cm². For electron temperatures not less than 0.5 keV, such fluxes are definitely above the threshold for the excitation of two of the above parametric instabilities in the polyethylene plasma ($t \to l + s$ and $t \to l + l$). When, on the other hand, the light fluxes are such that the electron temperature in the laser plasma is greater than 0.8 keV (Fig. 4), all three potential parametric instabilities ($t \to l + a$, $t \to l + s$, $t \to l + l$) are developed in the polyethylene plasma (see Fig. 6 for the maximum growth rates which determine the characteristic para-metric growth times). In the aluminum plasma, the threshold fluxes are somewhat higher because of the larger values of z (see Figs. 5 and 7).

The oscillatory character of the reflected flux as a function of time may be associated with the fact that the time-dependent turbulent parametric noise, which is established as a result of the development of one of the parametric instabilities, is cut off in time (by the re-laxation oscillations). This idea is qualitatively con-firmed and illustrated in Fig. 10 which gives the energy per unit volume for parametric turbulence initiated by the parametric instability involving the decay of the light wave into two high-frequency potential electron
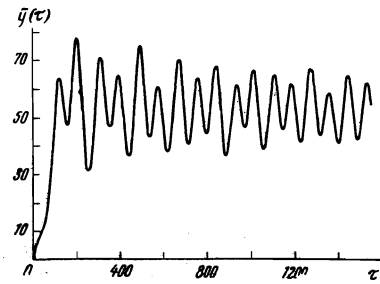

FIG. 10. Theoretical energy density of parametric turbulence initiated by a strong light beam in laser plasma at density equal to approxi-mately one quarter of the critical value for the neodymium laser. The horizontal axis gives the dimensionless time $\tau = 2\nu_{ei}t$ (ν_{ei} is the frequency of Coulomb collisions between electrons and ions) and the vertical axis gives the dimensionless energy $\bar{y}(\tau)$ of parametric turbulence per unit volume which is related to the electric field E in the plasma waves by (2).

oscillation.[19] This figure shows the $\bar{y}(\tau)$ curve ob-tained by analytical and numerical solution of the non-linear integrodifferential equation for the spectral en-ergy density $W(k, t)$ of the plasma noise with wave vector k:

$$\frac{\partial}{\partial t} W(k, t) = S(k) + 2\gamma(k) W(k, t) - W(k, t) \int dk' Q(k, k') W(k', t), \quad (1)$$

$$\frac{E^2}{8\pi} = 2 \int \frac{dk}{(2\pi)^3} W(k, t) \approx 15\bar{y}(\tau) z^2 A \frac{T_e^{5/2}}{T_i^2} \left(1 + \frac{T_i}{zT_e}\right)^2 (1 + 0.3 \lg T_e)$$

$$\times \left[1 - \left(\frac{q_{th}}{q}\right)^{1/2}\right]^2 \left(\frac{q}{q_{th}}\right)^{1/2} [J/cm^3], \quad (2)$$

which grows from the thermal level $S(k)/\nu_{ei}$ due to the parametric instability with a growth rate $\gamma(k)$ [the second term on the right-hand side of (1)] and is satu-rated by stimulated scattering on ions with cross sec-tion $Q(k, k')$ [third term on the right of (1)]. In these expressions E is the electric field in the high-frequency electron wave, z is the ion charge in the laser plasma, A is the atomic number, T_e and T_i are the electron ion temperatures in keV, and n_e is the density in cm^{-3}. The dimensionless time is given by

$$\tau = 0.3 z T_e^{-1/2} (q/q_{th})^{1/2} t,$$

where t is in psec.

The time taken by the plasma noise to increase to the turbulent value is determined by the time for the devel-opment of the parametric instability ($t \to l + l$; see Figs. 6 and 7) multiplied by the logarithm of the ratio of the turbulent noise to the spontaneous noise (roughly a factor of 10):

$$t_r \approx 0.1 \frac{T_e^{1/2}}{z} (1 + 0.3 \lg T_e) \left\{1 + 0.2 \lg\left[zA \frac{T_e^{5/2}}{T_i^2} \left(1 + \frac{T_i}{zT_e}\right)^2\right.\right.$$

$$\left.\left. \times \left(\left(\frac{2.5 \cdot 10^{20}}{n_e}\right)^{1/2} - 1\right)^{-1/2}\right]\right\} [nsec] \quad (3)$$

Since this time is shorter by more than an order of magnitude than the length of the laser pulse, even at laser plasma temperature of a few keV, a high level of turbulent parametric noise is established under our ex-perimental conditions.

The distribution shown in Fig. 10 is typical for the time relaxation of parametric turbulence in isotropic plasma, with induced scattering of oscillations by ions as the mechanism of saturation, and in general correctly illustrates the behavior of the high-frequency potential noise for other parametric instabilities which develop near the critical plasma density ($t \to l + a$, $t \to l + s$). It may therefore be assumed that the transformation of turbulent noise generated by the incident light beam into

a light wave leads to oscillations in the pulse reflected by the laser plasma, which are similar to the oscillations in the energy of potential oscillations in Fig. 10. The low efficiency of this transformation ensures that the absorption coefficient is high and, correspondingly, the reflection coefficient (re-radiation coefficient) is small. When this re-radiation of light by turbulence can be completely neglected, we can as before speak of the modulation of the signal reflected by the plasma with the modulation period of the turbulent noise (Fig. 10), since the pulsating level of turbulence leads to the modulation of anomalous absorption of the strong radiation and hence to a modulation of the reflection coefficient.

The curve shown in Fig. 10 is a theoretical result obtained on the assumption that the amplitude of the light wave incident on the plasma is independent of time, and without taking into account the spreading of the plasma, the shape of the incident pulse (Fig. 9b), and its finite length. Since allowance for these factors leads only to a slow (in comparison with the period of the oscillations) adiabatic variation in the mean time-independent level, it may be supposed that, for the incident pulses shown in Fig. 9b, the turbulent noise of the kind illustrated in Fig. 10 will be very similar to the structure of the reflected pulse (Fig. 9a). We may therefore consider that there is a qualitative agreement between the experimental data shown in Fig. 9a and the theoretical representation illustrated in Fig. 10.

It is important to emphasize that quantitative comparison of the periods and amplitudes of the oscillations in Fig. 9a and Fig. 10 will require more specific information about the properties of parametric turbulence and more complete experimental data. In particular, it follows from the nonlinear theory of parametric resonance that the period T of the oscillations in Fig. 10 is very dependent on the excess of the strong light flux above the threshold value, the plasma electron temperature, the mass of the ions, and so on:

$$T \approx 0.2 \left(\frac{T_e T_i}{A z^2} \right)^{1/4} \left[1 - \left(\frac{q_{th}}{q} \right)^{1/4} \right]^{-3/4} \left(\frac{q_{th}}{q} \right)^{1/4} [\text{nsec}], \qquad (4)$$

and therefore the experimental detection of such details would provide a more complete answer to the question as to what is the physical mechanism responsible for the oscillations in the signal reflected by the plasma. We emphasize also that the success of such a quantitative comparison would provide a means of laser plasma diagnostics. In particular, if we measure the period T of the light intensity reflected by laser plasma with ion charge z and atomic number A we can use (4) to determine the ion temperature T_i from known flux density q and the corresponding electron temperature $T_e \sim q^{4/9}$.
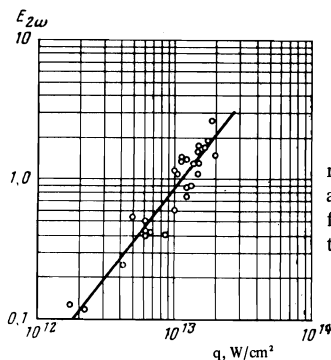

FIG. 11. Measured second-harmonic energy $E_{2\omega}$ within the solid angle of the lens as a function of the flux density q of light incident on the plasma.

As indicated in the first part of this section, the light pulse reflected by the laser plasma exhibits another characteristic feature which has been established experimentally, namely, the reduction in the width of the leading front by a factor of about 2.5 as compared with the leading front of the incident pulse. For turbulent noise this reduction in the width of the leading front may be explained in terms of Fig. 10 by the short time taken by turbulence, which re-radiates the plasma light, to reach its final level [see (3)].

4. GENERATION BY LASER PLASMA OF INCIDENT-LIGHT HARMONICS

In this Section we describe experimental results on light re-radiated by laser plasma at frequencies exceeding the incident frequency by factors of 1.5 and 2. These data are then interpreted theoretically.

We have examined experimentally the flux density q_2 in the second harmonic of the neodymium laser radiation (wavelength $\lambda = 5300$ Å), which appears in the spectrum of the radiation reflected by the plasma ($\lambda = 10\,600$ Å), as a function of the incident flux density q. The measurements were performed with the ISP-51 spectrograph and the UF-89 camera. Solid aluminum and polyethylene targets were employed and the incident flux density was varied between 2×10^{12} and 2×10^{13} W/cm^2.

The experimental dependence of the second-harmonic energy on the incident flux density q is shown in Fig. 11. The energy of the second harmonic when the flux density at the fundamental frequency was $q \approx 10^{13}$ W/cm^2 was taken as the unit of the second-harmonic energy, which amounted to about 10^{-4} of the energy incident on the plasma. The flux density q_2 in the second harmonic is related to the flux density q at the fundamental frequency by the formula $q_2 \sim q^\alpha$ where $\alpha = 1.4 \pm 0.1$. No differences were found between the second-harmonic radiation for the aluminum and polyethylene targets.

Generation of the second harmonic by laser plasma can be interpreted theoretically as the result of coalescence of potential electron Langmuir oscillations excited in the plasma by incident radiation and the light wave reflected from the critical density $(t + l \rightarrow t)$, or as the result of the coalescence of two electron Langmuir oscillations $(l + l \rightarrow t)$. The mechanism responsible for the excitation of the electron Langmuir oscillations by the incident light may take different forms. For low enough light fluxes $q \leq q_{th}$, which do not exceed the threshold value q_{th} necessary for parametric excitation of oscillations, the potential electric field is found to increase in the neighborhood of the critical density in inhomogeneous plasma because of the linear transformation of p-polarized light waves into electron Langmuir oscillations on the gradient of the plasma density.[20] It is precisely this mechanism of excitation of plasma waves which was used in papers devoted to the theory of second-harmonic generation.[21-23]

According to[22], the flux of radiation from laser plasma at the second-harmonic frequency is determined by different relationships depending on the type of coalescing waves $(t + l \rightarrow t$ or $l + l \rightarrow t)$ and the angle of incidence θ on the plasma. Taking the electron temperature of the plasma in the form $T_e \sim q^{4/9}$ (see the reviews in[24,25]), we find that the second-harmonic flux density q_2 increases with increasing incident flux

density q more slowly than q^2, in accordance with the experimental curve in Fig. 11:

$$t+l \rightarrow t: \quad q_2 \infty q^{46/27} \approx q^{1.70}, \quad \theta > \theta_0,$$
$$t+l \rightarrow t: \quad q_2 \infty q^{40/27} \approx q^{1.48}, \quad \theta < \theta_0,$$
$$l+l \rightarrow t: \quad q_2 \infty q^{26/27} \approx q^{0.96}.$$

In these expressions θ_0 is the critical value of the angle of incidence on the plasma, which is determined by the plasma temperature (see[22] for further details). It is clear from these formulas that the theoretical value of the exponent is not exactly the same as the experimental result, although the two are quite close to one another: one of these gives $\alpha = 1.48$ and this lies in the range $\alpha = 1.3-1.5$ which takes in the points in Fig. 11. If the second-harmonic generation is in fact due to the mechanism proposed above, the spread in the values of the exponent α round the experimental value $\alpha = 1.4 \pm 0.1$ is probably an indication of the fact that the $t + l \rightarrow t$ coalescence of the light wave (t) reflected from the critical density and the electron Langmuir oscillation (l) at small angles of incidence is the dominant process.

The fact that no differences were noted in the behavior of the second harmonic for different targets is an indication that the mechanism responsible for the generation of the second harmonic is of purely electronic origin, which is not inconsistent with the theory.[21-23]

For light flux densities q exceeding the threshold value for the excitation of parametric instability, $q \geq q_{th}$, the energy density of the high-frequency potential oscillations in the plasma reaches the turbulent level which is quite sufficient for the generation of the second harmonic even in homogeneous plasma where effects connected with the finite size of inhomogeneity in the density profile have either no influence or are very small. At the same time, the second harmonic may be generated by the plasma due to parametric instabilities of the form $t \rightarrow l + a$, $t \rightarrow l + s$ which develop in the neighborhood of the critical density of the laser plasma. The fact that there are special directions for the optimum development of parametric turbulence, relative to the polarization vector of the light wave and its wave vector, enables us to determine the directions of preferred second-harmonic generation for this mechanism. If in the above mechanism of second-harmonic generation on the plasma density gradient the emission at twice the frequency propagates in the direction opposite to that of the incident light beam, the parametric generation of the second harmonic occurs largely in the direction of the polarization vector of the incident light wave (for a small excess of the light flux above the threshold value). It is important to note, however, that for very high light flux densities, $q \gg q_{th}$, the parametric generation leads to an increase up to 180° in the angle at the apex of the two-sheet cone of second-harmonic emission (with axis along the electric vector in the incident light wave), so that the $\lambda = 5300$ Å line should be observed in practically the entire half-space in front of the target.

In addition to the second harmonic, the spectrum reflected into the collecting solid angle of the focusing lens for incident flux densities $q \approx 10^{13}$ W/cm² was found to contain the $\lambda \approx 7066$ Å line which corresponds to a frequency exceeding the incident frequency by a factor of 1.5 (cf.[26]). The signal-to-noise ratio for this line was much smaller than for the second harmonic

($\lambda = 5300$ Å). The origin of this line in the spectrum of the light re-radiated by the laser plasma can be understood in terms of the above idea of parametric generation of harmonics of the incident radiation. In fact, the $t \rightarrow l + l$ parametric instability, involving the decay of the light wave into two electron oscillations, develops at plasma densities equal to approximately one quarter of the critical density and generates plasma waves with frequency equal to one-half of the incident light wave frequency ω_0. The coalescence ($\omega_0/2 + \omega_0$) of the potential plasma oscillation with the wave reflected from the critical density in the plasma gives the observed line at $\frac{3}{2}\omega_0$. Moreover, it is important to note that the role of the reflected light wave, which as indicated above coalesces with the plasma wave, may be taken up by the Stokes component of SMBS. In both cases, the harmonic of frequency $\frac{3}{2}\omega_0$ is generated in the region of the plasma with density equal to one quarter of the critical value.

These variants of the parametric generation of light with frequency $\frac{3}{2}\omega_0$ by the plasma, which exceeds the neodymium-laser frequency by a factor of 1.5, lead to different angular distributions of the $\frac{3}{2}\omega_0$ radiation.

CONCLUSION

The anomalous interaction between strong laser radiation and dense plasma, which was discussed above, appears in the form of three effects, namely, the almost complete absorption of incident light by the plasma, the oscillation in the intensity of radiation reflected by the plasma as a function of time, and the generation of harmonics of the incident radiation. The interpretation of these experimental results within the framework of the theory of parametric resonance has enabled us not only to achieve a better understanding of their physical nature, but has also revealed further ways of investigating the anomalous interaction with a view to achieving optimum parameters for the laser + plasma system under conditions approaching the thermonuclear situation.

In this connection, we emphasize the diagnostic importance of measurements of the period and depth of modulation of reflected intensity as a means of independent determination of the temperature of the laser plasma. The measured dependence of the period of these oscillations on the charge z and atomic number A of the ions should enable us to determine the mechanisms of excitation and saturation of parametric turbulence which will be the most effective in laser plasma and could be used for heating purposes.

Comparison of the results of laser experiments with the predictions of the theory of parametric resonance shows that the idea of parametric instabilities does enable us to understand the particular effects associated with the interaction between strong light fluxes and high-temperature laser plasmas. These effects include not only strong absorption, modulation of reflected intensity, and generation of harmonics, but also the quasilinear parametric acceleration of plasma particles by the turbulence fields. Hard x-ray emission is determined by fast electrons, while the spectrum of fast ions should affect neutron measurements.

The light fluxes of $2 \times 10^{12}-2 \times 10^{13}$ W/cm², employed in the present work, lie near the threshold values for the excitation of parametric instabilities for which Coulomb

collisions between electrons and ions (collisional absorption) are still important. For light flux densities well in excess of the threshold value, $q \gg q_{th}$, absorption is completely determined by parametric turbulence (as in the case of strong microwaves[27]), and the dependence of the mean energy of electrons in laser plasma on the flux density is different from that determined by collisional absorption, i.e., $T_e \sim q^{4/9}$.

The authors are indebted to V. A. Kovalenko for assistance in the adjustment of the photoelectric recorder.

[1] N. G. Basov and O. N. Krokhin, Zh. Eksp. Teor. Fiz. 46, 171 (1964) [Sov. Phys.-JETP 19, 123 (1964)].

[2] N. G. Basov and O. N. Krokhin, Vestnik AN SSSR 6, 55 (1970).

[3] Yu. V. Afanas'ev, N. G. Basov, P. P. Volosevich, O. N. Krokhin, E. I. Levanov, V. B. Rozanov, and A. A. Samarskii, Preprint FIAN SSSR, No. 66 (1972).

[4] J. Nuckolls, L. Wood, A. Thiessen, and G. Zimmerman, Nature 239, 139 (1972).

[5] K. A. Brueckner and S. Jorna, Laser driven fusion, KMSF-U97, Michigan, USA, 1973.

[6] N. G. Basov, O. N. Krokhin, G. V. Sklizkov, S. I. Fedotov, and A. S. Shikanov, Zh. Eksp. Teor Fiz. 62, 203 (1972) [Sov. Phys.-JETP 35, 109 (1972)].

[7] N. G. Basov, Yu. S. Ivanov, O. N. Krokhin, Yu. A. Mikhailov, G. V. Sklizkov, and S. I. Fedotov, ZHETF Pis. Red. 15, 589 (1972) [JETP Lett. 15, 417 (1972)].

[8] V. D. Dyatlov, R. N. Medvedev, V. N. Sizov, and A. D. Starikov, ZhETF Pis. Red. 19, 124 (1974) [JETP Lett. 19, 76 (1974)].

[9] A. A. Rupasov, G. V. Sklizkov, V. P. Tsapenko, and A. S. Shikanov, Zh. Eksp. Teor. Fiz. 65, 1898 (1973) [Sov. Phys.-JETP 38, 947 (1974)].

[10] A. A. Rupasov, V. P. Tsapenko, and A. S. Shikanov, Preprint FIAN SSSR, No. 94 (1972).

[11] V. P. Silin, Zh. Eksp. Teor. Fiz. 48, 1679 (1965) [Sov. Phys.-JETP 21, 1127 (1965)]; Ukr. Phys. J. 108, 625 (1972); Preprint FIAN SSSR, Nos. 62 and 84 (1973).

[12] V. P. Silin, Parametricheskoe vosdeistvie izlucheniya bol'shoi moshchnosti na plazmu (Parametric Interaction Between High-intensity Radiation and Plasma), Nauka, 1973.

[13] N. E. Andreev, A. Yu. Kiriĭ, and V. P. Silin, Zh. Eksp. Teor. Fiz. 57, 1024 (1969) [Sov. Phys.-JETP 30, 559 (1970).

[14] L. M. Gorbunov, Zh. Eksp. Teor. Fiz. 55, 2298 (1968) [Sov. Phys.-JETP 28, 1220 (1969)].

[15] N. E. Andreev, Zh. Eksp. Teor. Fiz. 59, 2105 (1970) [Sov. Phys.-JETP 32, 1141 (1971)].

[16] R. R. Ramazashvili, Zh. Eksp. Teor. Fiz. 53, 2168 (1967) [Sov. Phys.-JETP 26, 1225 (1968)].

[17] V. P. Silin and A. N. Starodub, Zh. Eksp. Teor. Fiz. 66, 176 (1974) [Sov. Phys.-JETP 39, 82 (1974)] Preprint FIAN SSSR, No. 124 (1973).

[18] V. V. Pustovalov and V. P. Silin, Zh. Eksp. Teor. Fiz. 59, 2215 (1960; [Sov. Phys.-JETP 32, 1198 (1971)]; Kratkiye soobscheniya po fizike (Brief Communications on Physics) 8, FIAN, 1972, p. 33.

[19] N. E. Andreev, V. V. Pustovalov, V. P. Silin, and V. T. Tikhonchuk, Pis. Red. ZhETF 18, 624 (1973) [Sov. Phys.-JETP 18, 366 (1973)].

[20] V. L. Ginzburg, Rasprostranenie élektromagnitnykh voln v plazme (Propagation of Electromagnetic Waves in Plasma), Nauka, 1967.

[21] N. S. Erokhin, V. E. Zakharov, and S. S. Moiseev, Zh. Eksp. Teor. Fiz. 56, 179 (1969) [Sov. Phys.-JETP 29, 101 (1969)].

[22] A. V. Vinogradov and V. V. Pustovalov, Zh. Eksp. Teor. Fiz. 63, 940 (1972) [Sov. Phys.-JETP 36, 492 (1973)].

[23] N. S. Erokhin and S. S. Moiseev, Zh. Tekh. Fiz. 40, 1144 (1970) [Sov. Phys.-Tech. Phys. 15, 885 (1970)]; Voprosy teorii plasmy (Problems in Plasma Theory), cited by M. A. Leontovich 7, Atomizdat, 1973, p. 146.

[24] O. N. Krokhin, High-temperature and plasma phenomena induced by laser radiation. Physics of High Energy Density, XLVIII Corso, 1971.

[25] V. A. Boiko, O. N. Krokhin, and G. V. Sklizkov, Preprint FIAN SSSR, No. 121 (1972); Trudy FIAN SSSR 76 (1974).

[26] J. L. Bobin, M. Decroisette, B. Meyer, and Y. Vitel, Phys. Rev. Letters 30, 594 (1973).

[27] I. R. Gekker, Preprint FIAN SSSR, No. 132 (1973).